Synthesis and antibacterial activity of silver/reduced graphene oxide nanocomposites against *Salmonella typhimurium* and *Staphylococcus aureus*

Minh Dat Nguyen[1], Vu Duy Khang Pham[2], Le Phuong Tam Nguyen[1], Minh Nam Hoang[1, 2], Huu Hieu Nguyen[1, 2*]

[1]*Faculty of Chemical Engineering, Ho Chi Minh city University of Technology, Vietnam National University, Ho Chi Minh city*
[2]*Key Laboratory of Chemical Engineering and Petroleum Processing, Ho Chi Minh city University of Technology, Vietnam National University, Ho Chi Minh city*

Received 5 March 2018; accepted 4 June 2018

Abstract:

In this study, silver/reduced graphene oxide (Ag/rGO) nanocomposites were synthesized *in situ* using three different mass ratios of silver nitrate and graphene oxide (1:1, 2:1, and 4:1). L-ascorbic acid (LAA) was used as an environment-friendly reducing agent. The characterization of Ag/rGO was investigated using Fourier transform infrared spectroscopy, X-ray diffraction, Raman spectroscopy, and transmission electron microscopy. The investigated results showed that the Ag/rGO nanocomposites were successfully synthesized with silver nanoparticles in the size range of 10-25 nm uniform distribution on rGO sheets. The antibacterial activity of Ag/rGO was tested against Gram-negative (*Salmonella typhimurium)* and Gram-positive (*Staphylococcus aureus*) bacteria using plate colony-counting and broth dilution methods, in comparison with individual rGO and silver nanoparticles. The tested results showed that the Ag/rGO nanocomposite with the $AgNO_3$:GO ratio of 4:1 (Ag/rGO4:1) exhibited the strongest antibacterial activity. The minimal inhibitory concentration values of Ag/rGO4:1 against *Salmonella typhimurium* and *Staphylococcus aureus* were 10 µg/ml and 50 µg/ml, respectively. Hence, the Ag/rGO nanocomposite could be considered as a potential antibacterial agent.

Keywords: **nanocomposite, *Salmonella typhimurium*, silver/reduced graphene oxide, *Staphylococcus aureus*.**

Classification number: **5.2**

Introduction

In spite of the advanced developments in drug discovery and biotechnology, people continue to be affected annually by bacterial infection, making it one of the world's public health concerns. Conventional antibacterial drugs are commonly used to address the problem. However, the overuse of antibiotics and drugs has led to bacterial resistance [1]. Therefore, various antibacterial agents, such as carbon nanotubes, metal oxide nanoparticles [2], graphene-based materials [3], and metal nanoparticles [4], have been studied to resolve the issue.

Graphene oxide (GO) is a two-dimensional material that consists of a single layer of carbon atoms arranged in honeycomb network. Each carbon atom forms three covalent bonds with three other carbon atoms by sp^2 hybridization, creating a hexagonal structure with electron-rich π-π conjugation system [5]. GO was fabricated oxidizing graphite to form graphite oxide (GiO), followed by exfoliation; thus, it contains various oxygenated functional groups on the surface and edges, such as hydroxyl (OH), epoxy (-O-), cacbonyl (-C=O), and carboxylic (-COOH) [6, 7]. Similar to GO, reduced graphene oxide (rGO) is also a two-dimensional material but has few oxygenated functional groups on its basal plane or in its structure. It can be synthesized by the chemical reduction of GO [8, 9]. rGO is applied in many different fields, such as biology [6], nanoelectronics [7], energy storage devices, and water purification [8, 9]. Recently, the antibacterial activity of rGO has been widely researched due to the physical contact between rGO and the bacteria cell wall. rGO sheets with around 1 nm in diameter are capable of both deteriorating bacteria membrane integrity and surrounding the bacteria due to their electron-rich surfaces [2]. However, rGO

*Corresponding author: Email: nhhieubk@hcmut.edu.vn

antibacterial activity is relatively low due to the difficulty of fabricating single-layer rGO sheets and the fact that rGO sheets are easily accumulated. To enhance the antibacterial activity of rGO, metal nanoparticles or metal oxides have been employed to fabricate new nanocomposites. Among these, silver is commonly used owing to its potential antibacterial activity as compared with other metal nanoparticles or metal oxides and because it causes no harm to mammals [10]. AgNPs can easily release silver ions, generating reactive oxygen species (ROS), such as superoxide, hydrogen peroxide, or hydroxyl radicals [11]. Silver ions are capable of interacting with DNA, as DNA mostly contains sulfur and phosphorus, causing DNA replication malfunction and inhibiting bacteria growth [12].

The addition of silver in the fabrication of Ag/rGO leads to certain advantages: (1) It prevent the irreversible agglomerates due to strong π-π stacking tendency between reduced GO sheets; (2) reduces the thickness of rGO sheets; and (3) prevents aggregation of silver nanoparticles as the rGO sheets become substrates [13]. Therefore, the antibacterial activity of new fabricated nanocomposite could be relatively higher in relation to its precursors.

In this work, Ag/rGO nanocomposites were fabricated *in situ* with L-ascorbic (LAA) acid as a green reducing agent. The characterization of Ag/rGO was investigated by Fourier transform infrared spectroscopy (FTIR), X-ray diffraction (XRD), transmission electron microscopy (TEM), and Raman spectroscopy. Gram-negative bacteria, *Salmonella typhimurium* (*S. typhimurium)*, and Gram-positive bacteria, *Staphylococcus aureus* (*S. aureus*), were selected as model strains to study the antibacterial properties of the nanocomposites.

Materials and methods

Materials

Graphite powder (D_h<20 μm) was obtained from Sigma-Aldrich, Germany. Potassium permanganate ($KMnO_4$, 99%), ammoniac (NH_4OH), ethanol (C_2H_5OH, 95%), and L-ascorbic acid ($C_6H_8O_6$, 99.7%) were purchased from ChemSol, Vietnam. Sulfuric acid (H_2SO_4, 98%), phosphoric acid (H_3PO_4, 86%), hydrogen peroxide (H_2O_2, 85%), chlohydric acid (HCl, 36%), silver nitrate ($AgNO_3$, 99.8%), poly (vinylpyrrolidone) (PVP, M_w=10,000), and sodium chloride (NaCl, 99.5%) were purchased from Xilong, China. Mueller-Hinton agar powder (500 g) and Luria-Bertani (LB) powder were purchased from Himedia, India. All chemicals were analytical grade and used as received without performing any further purification.

Synthesis of GO

GO was prepared from graphite powder using the improved Hummers method [14]. 3 g of graphite powder was slowly added to the mixture of 360 ml of H_2SO_4 and 40 ml of H_3PO_4 in a 1,000 ml beaker. Then, 18 g of $KMnO_4$ was added into the mixture, followed by a 30-minute stirring in an ice bath. The mixture was stirred and heated to 50°C for 12h. Then, the mixture was cooled to room temperature and slowly diluted with 500 ml of distilled water. 15 ml of H_2O_2 was added and the colour of the solution changed from brown to yellow. The mixture was centrifuged and washed with HCl, distilled water, and ethanol, respectively, until the pH reached 6. The solid was dried at 50°C for 24h in order to obtain GiO.

GiO was then dispersed in distilled water to form a GO suspension by sonication for 12h.

Synthesis of rGO

The rGO was synthesized by the chemical reducing method [15]. First, 40 ml of LAA (4 mg/ml) was added into 10 ml of GO (4 mg/ml). The mixture was stirred and heated to 95°C for 2.5h. After that, the mixture was cooled to room temperature. The resulting mixture was centrifuged and washed with deionized water and ethanol, respectively, until pH of the wastewater reached 7, and dried at 60°C. The rGO powder was obtained.

Synthesis of silver/ammonia solution ($AgNO_3/NH_3$)

$AgNO_3/NH_3$ was prepared by dissolving 2 g of silver nitrate in 450 ml water, then adding aqueous ammonia solution into the silver nitrate solution under continuous stirring until the brown precipitates disappeared. The mixture was adjusted to a final volume of 500 ml with water. The concentration of $AgNO_3$ obtained in $AgNO_3/NH_3$ solution was about 4 mg/ml.

Synthesis of silver nanoparticles (AgNPs)

AgNPs was synthesized using the chemical reducing method in a PVP environment [16]. First, 32 mg of PVP was dispersed in 10 ml $AgNO_3/NH_3$ (4 mg/ml). Then, 5 ml of LAA (4 mg/ml) was added. The mixture was stirred and heated to 95°C for 2.5h. Thereafter, the solution was cooled to room temperature. The resulting mixture was centrifuged and washed with deionized water and ethanol, respectively, until the pH of the wastewater reached 7, and then it was dried at 60°C. The AgNPs powder was obtained.

Synthesis of Ag/rGO nanocomposites

The Ag/rGO nanocomposites were synthesized using an *in-situ* method, in which both silver nitrate and GO were reduced simultaneously using LAA as a green reducing agent. The nanocomposites prepared from different mass ratio of $AgNO_3$:GO were labelled as Ag/rGO1:1, Ag/rGO2:1, and Ag/rGO4:1.

The $AgNO_3/NH_3$ solution was added into the GO solution. The mixture was sonicated for 20 minutes, after which, LAA was added. The mixture was stirred and heated to 95°C for 2.5h. The resulting mixture was centrifuged and washed with deionized water and ethanol, respectively, until the pH of the wastewater reached 7, and then it was dried at 60°C to obtain Ag/rGO. The volumes of reactants used to prepare corresponding samples are shown in Table 1.

Table 1. The volumes of reactants used to prepare corresponding samples (ml).

Samples	$AgNO_3/NH_3$ (4 mg/ml)	GO (4 mg/ml)	LAA (4 mg/ml)
Ag/rGO1:1	10	10	45
Ag/rGO2:1	10	5	25
Ag/rGO4:1	10	2.5	15

Characterization

The XRD patterns of GO, rGO, and Ag/rGO were studied using XRD D2 Pharser machine (Bruker AXS, Germany) with Cu Kα radiation (λ=0.154 nm). FTIR spectra of GO, rGO, and Ag/rGO were performed by the Tensor 27 FTIR spectrophotometer (Bruker, Germany). The TEM images were obtained using the JEM 1400 microscope (JEOL, Japan) at an acceleration voltage of 100 kV. Raman spectroscopy was obtained by using LabRam HR Evolution (Horiba, Japan) with an excitation wavelength of 632 nm (He-Ne laser).

Antibacterial test

The antibacterial activities of nanocomposite materials and precursors were tested using plate colony-counting method in order to identify the material with the strongest antibacterial potential. The minimal inhibitory concentration (MIC) of the material was determined by dilution. *S. typhimuriu* and *S. aureus* were obtained from Faculty of Biology and Biotechnology, HCMUS and incubated at 37°C in LB.

Plate colony-counting method: antibacterial agents (rGO, AgNPs, and Ag/rGO) were added to 20 ml of the bacterial suspension at a concentration of 200 mg/ml. The mixture was shaken constantly at 37°C for 6h. 0.1 ml of the diluted solution was uniformly spread in the solid medium in the agar plate and incubated at 37°C for 24h. The growth of the bacteria was observed by counting the total number of colonies per dish [13].

Broth dilution method: the antibacterial agents were added to 20 ml of the bacterial suspension at a concentration of 0.19 to 50 mg/l. The mixture was shaken constantly at 37°C for 24h. The resazurin 0.01% indicator was added. The color was blue at normal condition and changed to pink if there was bacterial growth. The MIC was determined using the test tube where the concentration was the lowest and the color of the solution remained blue.

Results and discussion

Characterization

FTIR spectra: the FTIR spectra of GO, rGO, Ag/rGO1:1, Ag/rGO2:1, and Ag/rGO4:1 are presented in Fig. 1. The distinctive diffraction peaks of GO at 3422 cm^{-1}, 1735 cm^{-1}, and 1400 cm^{-1} corresponded to the vibration of carboxylic (C=O), hydroxyl (C-OH), and epoxide (C-O-C), respectively [17]. These results confirmed the existence of oxygen-containing groups in the structure of the GO, indicating that graphite was successfully oxidized to GO. It can be seen from the FTIR spectra of rGO and Ag/rGO that there was a decrease in the intensity of characteristic peaks corresponding to oxygen-containing functional groups. This indicated that GO was reduced to rGO when using LAA as a green reducing agent [18, 19].

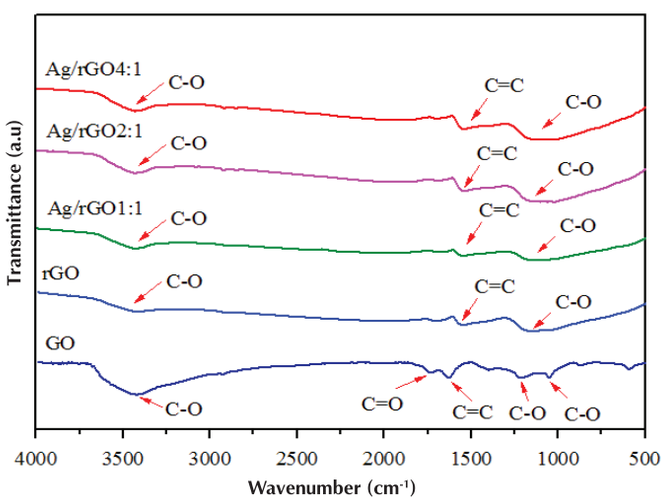

Fig. 1. The FTIR spectra of GO, rGO, Ag/rGO1:1, Ag/rGO2:1, and Ag/rGO4:1.

XRD patterns: the XRD patterns of GO, rGO, and Ag/rGO as shown in Fig. 2. GO exhibited a distinctive diffraction peak at $2\theta=9.6^0$, ascribing to (002) crystallographic plane with interlayer spacing $d_{(002)}=0.902$ nm. In the XRD pattern of rGO, there was no characteristic peak of GO but another peak at $2\theta=26^0$, indicating that GO has been was reduced successfully into rGO. The disappearance of the diffraction peak of GO can also be observed in the XRD patterns of Ag/rGO1:1, Ag/rGO2:1, and Ag/rGO4:1 fabricated materials. In addition, the distinctive diffraction peaks of silver nanoparticles can be clearly observed from the XRD patterns of Ag/rGO1:1, Ag/rGO2:1, and Ag/rGO4:1 at 2θ values of 38^0, 44^0, 64^0, and 77^0 ascribing to the crystallographic plane (111), (200), (220), and (311), respectively. These results confirmed the existence of silver in the structure of the Ag/rGO nanocomposites [20]. Besides, the disappearance of the characteristic peak of GO at $2\theta=26^0$ proved that the nanoparticles enhanced the interlayer spacing between rGO sheets.

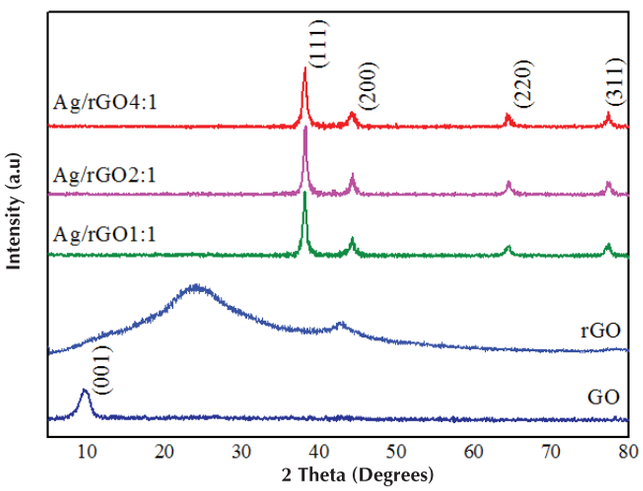

Fig. 2. XRD patterns of GO, rGO, Ag/rGO1:1, Ag/rGO2:1, and Ag/rGO4:1.

Raman spectroscopy: Raman spectra of GO, rGO, Ag/rGO1:1, Ag/rGO2:1, and Ag/rGO4:1 are presented in Fig. 3. G-band and D-band were approximately in the range of 1320-1335 cm^{-1} and 1585-1610 cm^{-1}, respectively [21]. The D-band is related to the disordered carbon and the G-band is associated with the in-plane stretching vibration of sp^2 C-C bonds [22]. The intensity ratio of the D-band and G-band (I_D/I_G) is referred to the structural imperfection of graphene-based materials. As shown in Fig. 4, the I_D/I_G ratios of GO and rGO were 1.05 and 1.19, respectively. These results showed that rGO had more defects than GO, indicating that GO was been reduced to rGO [21]. According to Fig. 4, the I_D/I_G ratios of Ag/rGO1:1, Ag/rGO2:1, and Ag/rGO4:1 were 1.20, 1.24, and 1.24, respectively, which were similar to that of rGO. This indicated that rGO was formed in the solution of silver ions during the fabrication of Ag/rGO.

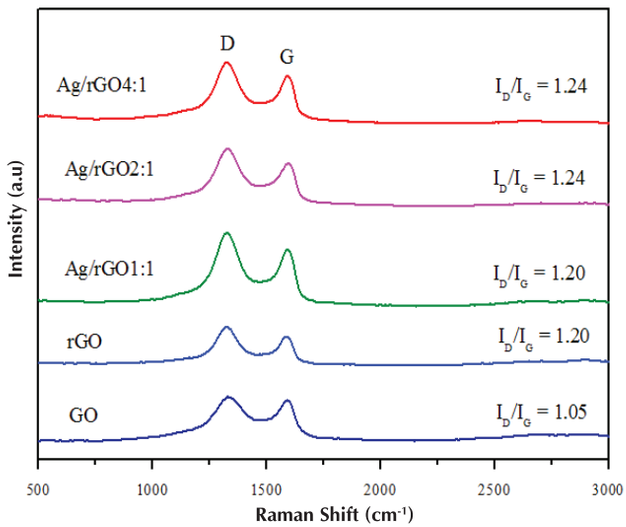

Fig. 3. Raman spectra of GO, rGO, Ag/rGO1:1, Ag/rGO2:1, and Ag/rGO4:1.

TEM images: TEM images of rGO, AgNPs, and Ag/rGO nanocomposites with different mass ratios of $AgNO_3$:GO are shown in Fig. 4. The light-gray thin films were rGO sheets [in Figs. 4(A, C, and E)] while black particles were silver nanoparticles. The results showed that with the presence of silver nanoparticles in the structure of rGO, there was also enhancement in the interlayer spacing between rGO sheets, which was indicated by the planar in Figs. 4(C, E), which was lighter than that in Fig. 4A. In Fig. 4B, the silver nanoparticles synthesized in PVP had the size range of 50 to 60 nm. Under the same synthesis conditions, upon replacing PVP with GO solutions, the silver nanoparticles synthesized and the size ranged from 15 to 25 nm, as shown in Figs. 4(C, E). The results were consistent with that of the previous study, as given in Table 2. This difference could be explained by the fact that rGO had high specific surface area along with many activated sites, which located the silver nanoparticles and prevented aggregation. The TEM images also showed that upon increasing the amount of $AgNO_3$, the amount of silver nanoparticles increased as well [17, 23].

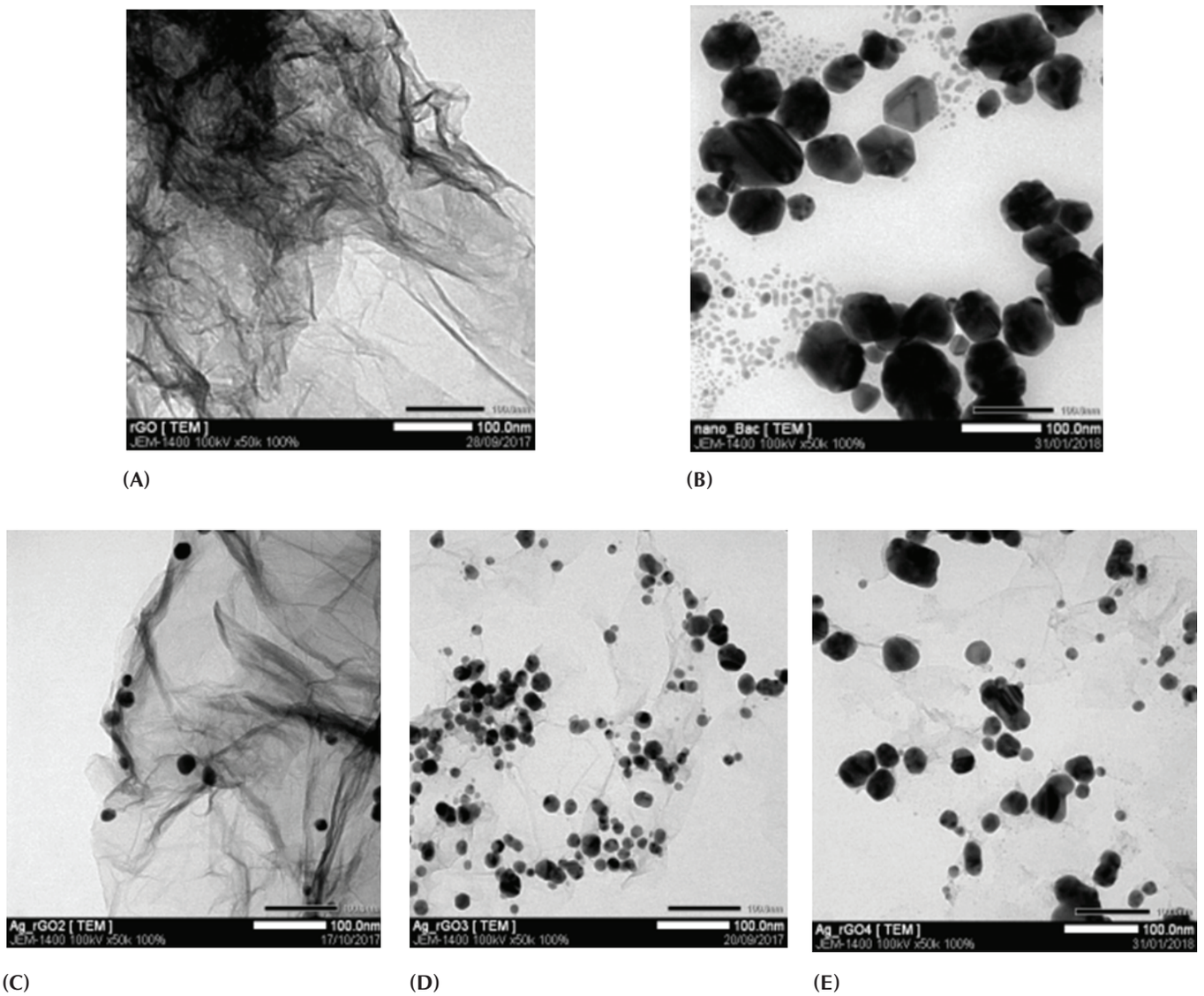

Fig. 4. TEM images of (A) rGO, (B) AgNPs, (C) Ag/rGO1:1, (D) Ag/rGO2:1, and (E) Ag/rGO4:1.

Table 2. The size of AgNPs (nm).

Materials	Size	References
Ag/rGO	15-25	Present work
AgNPs	50-60	Present work
Ag/rGO	20-50	[13]
Ag/GO	5-25	[23]
Ag/GO	22	[24]
AgNPs/PVP	69	[25]

Antibacterial activity evaluation

Antibacterial activity of fabricated materials: the antibacterial activities of rGO, AgNPs, and Ag/rGO nanocomposites with different mass ratios of $AgNO_3$:GO were evaluated by applying the plate colony-counting method. The antibacterial activity of each material depends on the number of colonies in each plate. The higher the number of colony in each plate, the lower the antibacterial activity of the sample was. The antibacterial activities of rGO, AgNPs, and Ag/rGO nanocomposites against *S. aureus* and *S. typhimurium* are presented in Fig. 5. The results showed that the materials showed higher antibacterial

activity against *S. typhimurium* rather than *S. aureus*. This could be explained by the fact that the cell wall of *S. aureus* was thicker than that of *S. typhimurium*; and hence, generated radicals could break the cell wall and decompose the inner parts of the cell. Among the tested materials, the Ag/rGO4:1 nanocomposite exhibited the strongest antibacterial potential owing to the highest amount of silver in Ag/rGO4:1. On the other hand, in the AgNPs sample, the large size of silver nanoparticles and the fact that they were covered by PVP resulted in the limitation of releasing silver ions.

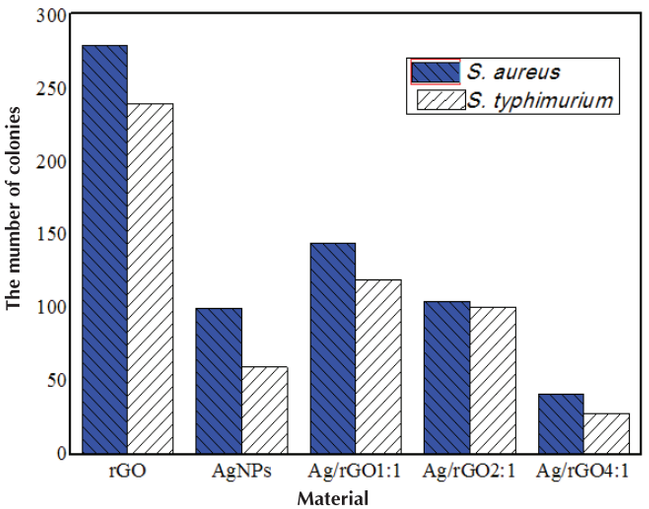

Fig. 5. The number of colonies of *S. aureus* and *S. typhimurium* in the presence of GO, rGO, Ag/rGO1:1, Ag/rGO2:1 and Ag/rGO4:1.

MIC value: the MIC value of Ag/rGO4:1 was determined using the broth dilution method, as shown in Fig. 6. According to this, the MIC values of Ag/rGO4:1 against *S. typhimuriu* and *S. aureus* were 10 mg/l and 50 mg/l, respectively. The higher MIC against *S. typhimurium* rather than *S. aureus* showed that *S. typhimurium* was more easily inhibited than *S. aureus*.

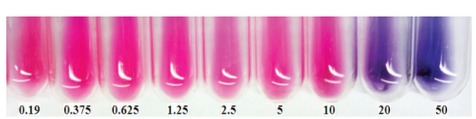

(A)

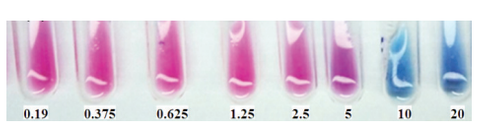

(B)

Fig. 6. Experiment to determine MIC of Ag/rGO4:1 against (A) *S. aureus* and *(B) S. Typhimuriu.*

Conclusions

The analysis results pertaining to XRD, FTIR, Raman, and TEM showed that Ag/rGO nanocomposites was fabricated successfully *in situ*. The silver nanoparticles in the size range of 10-25 nm were decorated uniformly on rGO sheets. The antibacterial test showed that the fabricated Ag/rGO had a strong antibacterial potential. Upon using more silver nitrate, the amount of silver nanoparticles increased, and hence, the antibacterial activity was enhanced. The Ag/rGO nanocomposites exhibited the strongest antibacterial activity, with the MIC value against *S. typhimuriu* and *S. aureus* being 10 mg/l and 50 mg/l, respectively. Therefore, it can be concluded that the fabricated Ag/rGO nanocomposite has great potential in antibacterial field.

REFERENCES

[1] L. Rizzello, P.P. Pompa (2014), "Nanosilver-based antibacterial drugs and devices: Mechanisms, methodological drawbacks, and guidelines", *Chem. Soc. Rev.*, **43**, pp.1501-1518.

[2] Shaobin Liu, Tingying Helen Zeng, Mario Hofmann, Ehdi Burcombe, Jun Wei, Rongrong Jiang, Jing Kong, Yuan Chen (2011), "Antibacterial Activity of Graphite, Graphite Oxide, Graphene Oxide, and Reduced Graphene Oxide: Membrane and Oxidative Stress", *ACS Nano*, **5(9)**, pp.6971-6980.

[3] Yong-WookBaek, Youn-JooAn (2011), "Microbial toxicity of metal oxide nanoparticles (CuO, NiO, ZnO, and Sb_2O_3) to Escherichia coli, Bacillus subtilis, and Streptococcus aureus", *Science of the Total Environment*, **409(8)**, pp.1603-1608.

[4] P.K. Vemula, P.M Ajayan, G. John A. Kumar (2008), "Silver-nanoparticles-embedded antimicrobial paints based on vegetable oil", *Nat. Mater.*, **7**, pp.236-241.

[5] S. Stankovich, D.A. Dikin, Geoffrey H.B. Dommett, Kevin M. Kohlhaas, Eric J. Zimney, Eric A. Stach, Richard D. Piner, SonBinh T. Nguyen, Rodney S. Ruoff (2006), "Graphene-based composite materials", *Nature*, **442**, pp.282-286.

[6] A.K Geim, S.V Morozov, E.M Hill, P. Blake, M.I Katsnelson, K.S Novoselov, F. Schedin (2007), "Detection of individual gas molecules adsorbed on graphene", *Nature Mater.*, **6**, pp.652-655.

[7] D.A Areshkin and C.T White (2007), "Building blocks for integrated graphene circuits", *Nano Lett.*, **7**, pp.3253-3259.

[8] P. Jain, T. Pradeep (2005), "Potential of silver nanoparticle-coated polyurethane foam as an antibacterial water filter", *Biotechnology and Bioengineering*, **90(1)**, pp.59-63.

[9] Dankovich (2011), "Bactericidal paper impregnated with silver nanoparticles for point-of-use water treatment", *Environ. Sci. Technol.*, **45(5)**, pp.1992-1998.

[10] S.W. Chook, C.H. Chia, S. Zakaria, and M.K. Ayob (2012), "Silver nanoparticles - graphene oxide nanocomposite for antibacterial purpose", *Advanced Material Research*, **364**, pp.439-443.

[11] Yang Li, Wen Zhang, Junfeng Niu, Yongsheng Chen (2013),

"Surface-coating-dependent dissolution, aggregation, and reactive oxygen species (ROS) generation of silver nanoparticles under different irradiation conditions", *Environ. Sci. Technol.*, **47(18)**, pp.10293-10301.

[12] David D. Evanoff Jr., George Chumanov (2005), "Synthesis and optical properties of silver nanoparticles and arrays", *Chem. Phys. Chem.,* **6(7)**, p.1221.

[13] Gu Danxia, Chang Xueting, Zhai Xinxin, Sun Shibin, Li Zhongliang, Liu Tao, Dong Lihua, Yin Yansheng (2016), "Efficient synthesis of silver-reduced graphene oxide composites with prolonged antibacterial effects", *Ceramics International*, **42(8)**, pp.9769-9778.

[14] Daniela C. Marcano, Dmitry V. Kosynkin, Jacob M. Berlin, Alexander Sinitskii, Zhengzong Sun, Alexander Slesarev, Lawrence B. Alemany, Wei Lu, James M. Tour (2010), "Improved synthesis of graphene oxide", *ACS Nano,* **4(8)**, pp.4806-4814.

[15] K.K.H. De Silva, H.H. Huang, R.K. Joshi, M. Yoshimura (2017), "Chemical reduction of graphene oxide using green reductants", *Carbon*, **119**, pp.190-199.

[16] Quang Huy Tran, Van Quy Nguyen, Anh Tuan Le (2013), "Silver nanoparticles: synthesis, properties, toxicology, applications and perspectives", *Adv. Nat. Sci.: Nanosci. Nanotechnol.*, **4**, p.033001.

[17] Jinlin Lu, Yanhong Li, Shengli Li, and San Ping Jiang (2016), "Self-assembled platinum nanoparticles on sulfonic acid-grafted graphene as effective electrocatalysts for methanol oxidation in direct methanol fuel cells", *Scientific Reports*, **6**, p.21530.

[18] Henan Zhang, Deon Hines, and Daniel L. Akins (2014), "Synthesis of a nanocomposite composed of reduced graphene oxide and gold nanoparticles", *Dalton Trans.*, **43**, pp.2670-2675.

[19] Tarko FentawEmiru and Delele WorkuAyele (2017), "Controlled synthesis, characterization and reduction of graphene oxide: A convenient method for large scale production", *Egyptian Journal of Basic and Applied Sciences*, **4(1)**, pp.74-79.

[20] Balwinder Kaur, Thangarasu Pandiyan, Biswarup Satpati, and Rajendra Srivastava (2013), "Simultaneous and sensitive determination of ascorbic acid, dopamine, uric acid, and tryptophan with silver nanoparticles-decorated reduced graphene oxide modified electrode", *Colloids and Surfaces B: Biointerfaces*, **111**, pp.97-106.

[21] J. Zhang, H. Yang, G. Shen, P. Cheng, and J. Zhang (2010), "Reduction of graphene oxide via L-ascorbic acid", *Chemical Communications*, **46(7**), pp.1112-1114.

[22] M. Zainy (2012), "Simple and scalable preparation of reduced graphene oxide-silver nanocomposites via rapid thermal treatment", *Materials Letters*, **89**, pp.180-183.

[23] Manash R. Das, Rupak K. Sarma, Ratul Saikia, Vinayak S. Kale, Manjusha V. Shelke, Pinaki Sengupta (2011), "Synthesis of silver nanoparticles in an aqueous suspension of graphene oxide sheets and its antimicrobial activity", *Colloids and Surfaces B: Biointerfaces*, **83**, pp.16-22.

[24] Wei Shao, Xiufeng Liu, Huihua Min, Guanghui Dong, Qingyuan Feng, Songlin Zuo (2015), "Preparation, characterization, and antibacterial activity of silver nanoparticle-decorated graphene oxide nanocomposite", *ACS Appl. Mater. Interfaces*, **7(12)**, pp.6966-6973.

[25] RasmusFoldbjerg, PingOlesen, MadsHougaard, Duy Anh Dang, Hans JürgenHoffmann, HermanAutrup (2009), "PVP-coated silver nanoparticles and silver ions induce reactive oxygen species, apoptosis and necrosis in THP-1 monocytes", *Toxicology Letters*, **190(2)**, pp.156-162.